2-D Soot Imaging in a Direct Injection Diesel Engine Using Laser-Induced Incandescence

A.O.zur Loye
Mail Code 50180
Cummins Engine Company
P.O. Box 3005
Columbus, IN 47202
U.S.A.

D.L.Siebers and J.E.Dec
Sandia National Laboratories

ABSTRACT

Laser-induced incandescence (LII) is being explored as a diagnostic for qualitatively imaging the distribution of soot in the cylinder of a diesel engine. A high energy light pulse from a frequency doubled Nd:YAG laser is formed into a sheet and introduced into the cylinder of an optically accessible diesel engine. Soot in the plane of the laser sheet is heated from diesel engine flame temperatures up to 4500 K. At wavelengths shorter than approximately 450 nm, the intensity of thermal emission from the laser-heated soot is much greater than that of the surrounding soot. Using spectral filters and an 80 ns gate on an intensified video camera, it is possible to record the image of the short wavelength emission from the high-temperature soot, while rejecting virtually all of the lower temperature thermal emission from the non-laser-heated soot surrounding the laser sheet, as well as any scattered 532 nm laser light. Preliminary soot distributions at various cylinder locations and crank angles in a 2.3 liter, single cylinder, direct injection diesel engine operating on number 2 diesel fuel have been recorded.

INTRODUCTION

Particulate and NO_x emissions standards for US on-highway heavy duty diesel engines are becoming more stringent in 1991, and even stricter in 1994. In order to build diesel engines that will meet these new standards, it is important that we improve our current limited understanding of the in-cylinder processes that lead to particulate and NO_x emissions from diesel engines.

One of the major reasons for our lack of understanding is a lack of diagnostic techniques for probing in-cylinder diesel engine combustion processes. The objective of this study is to explore the use of laser-induced incandescence (LII) as a method for generating qualitative images of the soot distribution in the cylinder of a diesel engine. Unlike soot imaging techniques based on elastic scattering, LII imaging makes it possible to obtain 2-D soot distributions in the presence of liquid fuel droplets, without interference from the droplets.

Laser-induced incandescence has been studied as a particle diagnostic [1] and as a noise source for other optical diagnostics [2]. Melton [3] performed an analysis of LII and discussed its potential for obtaining quantitative information about soot. The interaction of high energy laser pulses with soot has also been studied as a means for developing other new soot diagnostics [4-6]. While these earlier studies were concerned with single point measurements or theoretical developments, we have extended the use of LII to two dimensions. Specifically, we have used LII to obtain planar images of the soot distribution in the combustion chamber of a direct injection diesel engine at various crank angles and spatial locations. Obtaining a more accurate picture of when and where soot is formed during the diesel combustion cycle is essential to improving our understanding of the in-cylinder diesel soot formation processes.

PRINCIPLES OF 2-D LASER-INDUCED INCANDESCENCE IMAGING

Two-dimensional LII images are generated by collecting the thermal radiation from soot particles that have been heated by a sheet of pulsed laser light. Detailed analyses of the thermal response of soot particles to high intensity laser pulses [2,3,5] show that the rate of energy addition by the laser radiation is much greater than the energy losses due to transfer to the surrounding gas and thermal radiation. As a result, on time scales similar to the rise time of the laser pulse, the temperature of the soot is increased to a temperature near the vaporization temperature, after which the additional energy input from the laser is balanced by the energy of vaporization. Experimental measurements of laser-heated soot temperatures made by Eckbreth [2] and reproduced in Fig. 1 show that for laser intensities on the order of 10^7 W/cm^2 or greater, the surface temperature of the soot is about 4500 K and is in agreement with the theoretical vaporization curves. Depending on the intensity and duration of the laser pulse, the soot particles are either partially or completely vaporized, however, significant thermal emission occurs prior to vaporization [2,3].

*Work performed at the Combustion Research Facility at Sandia National Laboratories and supported by Cummins Engine Company and by the U.S. Department of Energy, Energy Conversion and Utilization Technologies Program.

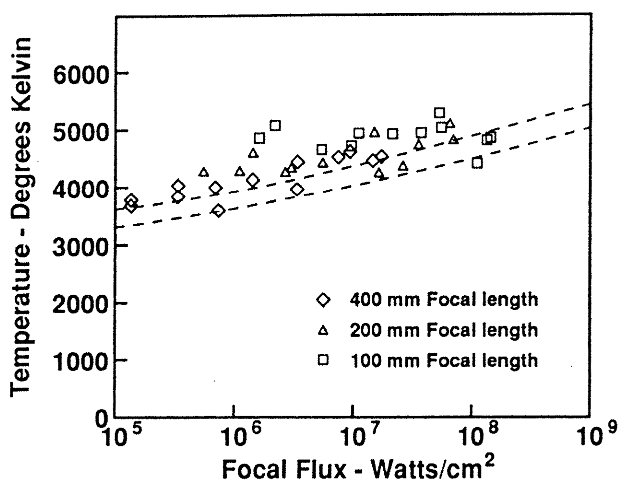

Figure 1 Laser induced soot surface temperature, as a function of laser focal flux using different focusing lenses. Dashed curves are analytical predictions. From Ref. [2].

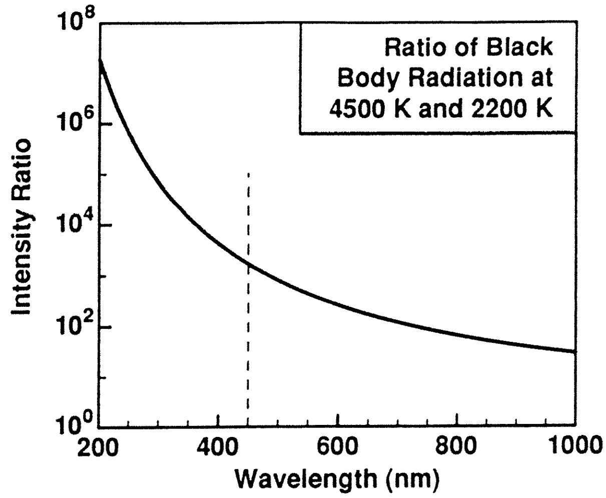

Figure 2 Ratio of black body radiation at 4500 K to that at 2200 K. Dashed line indicates cutoff wavelength of short wavelength pass filters.

Rejecting Background Luminosity

In the LII imaging technique the temperature difference between the laser-heated and non-laser-heated soot is exploited to reject the background luminosity from the soot not in the plane of the laser sheet. In a typical diesel engine, the temperature of non-laser-heated soot is on the order of 2200 K or less [7]. Assuming that soot emits thermal radiation as a gray body, we can compare the emission of 4500 K soot which lies in the path of the laser sheet to that of 2200 K soot outside the laser sheet. This comparison is presented in Fig. 2, where the ratio of these two emissive powers has been plotted on a logarithmic scale vs. wavelength. It can be seen that the laser-heated soot has a much higher emission at shorter wavelengths which provides the mechanism for rejecting the background luminosity.

Through the use of appropriate short wavelength pass filters, an image can be obtained of the thermal emission of the soot in the laser sheet. From Fig. 2, it can be concluded that the shorter the cutoff wavelength of this filter, the better the capability of rejecting unwanted luminosity. On the other hand, the overall intensity of the collected light will also decrease as the cutoff wavelength is reduced. For the measurements presented in this paper, a cutoff wavelength of 450 nm resulted in the best compromise between signal strength and rejection ability.

Background luminosity can be further suppressed by limiting the exposure time of the camera to the time during which the laser-heated soot is at an elevated temperature. After the laser pulse, the heated soot that has not vaporized will cool and its short-wavelength thermal radiation will decrease. Maximum background rejection would be achieved by limiting the exposure time to be on the order of the laser pulse duration (8 ns) [3]. For our experiment the shortest possible exposure time of our gated camera-intensifier system was about 80 ns, which was the exposure time used to obtain all the images for this study.

The ability to reject the background luminosity is critical for a successful application of 2-D LII imaging. There are four key factors that determine the rejection ability:

1) The temperature of the soot outside the laser sheet. The lower this temperature is, the better the rejection capability will be.
2) The ratio of the amount of soot inside the laser sheet to the total amount of soot in the field of view of the camera. The larger this ratio is, the better the rejection ability will be.
3) The cutoff wavelength of the optical filters in front of the camera. The shorter the cutoff wavelength, the better the rejection ability will be. Decreasing the cutoff wavelength, however, reduces the signal strength.
4) The exposure time of the camera. The closer this time is to the laser pulse duration, the better the rejection ability will be.

From this list, it can be seen that the rejection ability is determined to a large extent by the combustion process being measured. Fortunately it is easy to determine the magnitude of the background luminosity by acquiring images with the laser beam blocked. For all conditions studied, the background luminosity was found to be about the same magnitude as the dark noise of the camera system, which was negligible compared to the strength of the LII signals.

Rejecting Signals from Liquid Droplets

The primary advantage of laser-induced incandescence in diesel engines is that there is no interfering signal from fuel droplets that might be in the path of the laser sheet. Fuel droplets do not contribute significantly to the collected light for two reasons:

1) The light collected is at a wavelength that is much shorter than the laser wavelength. Elastic scattering, red-shifted laser-induced fluorescence, and red-shifted Raman scattering are easily suppressed.
2) Thermal emission from fuel droplets is insignificant. Because fuel drops are nearly transparent to the laser light, thermal heating is expected to be low. Moreover, the boiling point of the fuel is much lower than the

vaporization temperature of soot, so even if the fuel absorbs some incident laser light, it will evaporate before reaching temperatures at which thermal radiation becomes significant.

In order to confirm our ability to reject unwanted signals from fuel droplets, the engine was operated without preheating the intake air. At this operating condition, no combustion occurred, even though fuel was being injected. With the filters in place and the laser operating no signal from the fuel drops was detected.

Advantages and Disadvantages of Planar LII over Planar Elastic/Mie Imaging

The primary advantage of laser-induced incandescence over planar elastic/Mie imaging is the ability to obtain images of soot with no interfering signal from fuel droplets which might be in the path of the laser sheet. Another advantage is that the technique is insensitive to laser wavelength which allows effective suppression of elastically scattered light, laser-induced fluorescence, and Raman scattering from windows and other surfaces as well as fuel droplets.

The primary disadvantages of LII imaging are the difficulty of suppressing background luminosity, the lower (but adequate) signal strength, and the fact that this technique is partially intrusive. The technique is intrusive, because some of the soot is vaporized [3,5]. This could present a problem in an experiment where images are acquired in quick succession. In our experiment this was not an issue, because only one image was acquired in a particular engine cycle. It should be noted, that planar elastic/Mie imaging is typically performed with a high-powered pulsed laser also, and that the soot may still be vaporized.

Interpretation of 2-D Laser-Induced Incandescence Images

In principle, the qualitative interpretation of 2-D LII images is straight forward. Areas of high intensity in the image represent regions of high soot concentration, while areas of low intensity in the image represent regions of low soot concentration. Melton [3] predicts, that in the limit of high laser power the signal strength from laser-heated soot should be directly proportional to the local soot volume fraction. This analytical prediction has not been demonstrated experimentally, and it may not be possible to verify the necessary assumptions in the cylinder of a diesel engine. If the prediction proves to be correct, however, quantitative measurements may be possible in future applications.

As with most laser-based planar imaging techniques, interpretation of the LII images can be complicated by two key factors:

1) The intensity of the laser sheet will be attenuated by the soot as it travels across the image plane reducing the amount of laser power available for heating. This could either reduce, increase or have no effect on the incandescence signal depending on the laser intensity and soot density. If the incident laser intensity is barely sufficient to heat the soot in the near field to the vaporization temperature, attenuation will reduce the incandescence by reducing the temperature of the laser-heated soot in the far field. Alternatively, if the incident laser intensity is well above that required to reach the vaporization temperature, attenuation may only reduce the rate of vaporization of the soot in the far field and not its temperature. This could result in an increase in the incandescence from the far-field soot due to the larger size of the particles. Finally, if the laser power and pulse duration are sufficient, all the soot particles in the laser path (both near and far field) could be completely vaporized [3,5], and laser attenuation would have no effect.
2) Attenuation of the signal by soot between the laser sheet and the camera, signal trapping, can significantly reduce the LII signal. This could result in regions of high soot concentration showing up as low intensity areas in the image.

Both of these factors depend on the particular experiment, and their effect in our experiment is discussed in more detail in the results and discussion section.

EXPERIMENTAL SETUP

Optically Accessible Engine

A single cylinder Cummins NH diesel engine, modeled after a production NH/NT, direct injection, four stroke, 14 liter, six-cylinder engine was used for this study.

The specifications of the test engine are listed in Table 1, and a schematic of the engine's optical configuration is shown in Fig. 3. In order to gain optical access four major modifications were made to the engine:

Table I. Specifications of Optically Accessible Engine.

Type	Four-Stroke
Bore	14.0 cm (5.5 in)
Stroke	15.2 cm (6.0 in)
Displacement	2.34 ℓ (142 in^3)
Con-rod length	30.3 cm (12.0 in)
Compression ratio	12.5
Engine speed	600 rpm
Intake valve opening	30° BTDC
Intake valve closing	132° BTDC
Exhaust valve opening	139° ATDC
Exhaust valve closing	22° ATDC
Number of intake valves	2
Number of exhaust valves	1

1) A 3.81 cm (1.5 in.) thick steel spacing ring with four 3.02 cm (1.19 in.) diameter quartz windows was inserted between the head and the block.
2) A piston with modified valve cutouts producing a 12.5:1 compression ratio was used. This low compression ratio was compensated for by increasing the intake air temperature and pressure to 150° C and 2 bars absolute, respectively. To manufacture the piston, a stock piston was sliced into two pieces and discs were inserted between them to compensate for the larger cylinder height caused by the spacing ring. By changing the thickness of the discs the compression ratio could be modified. Two

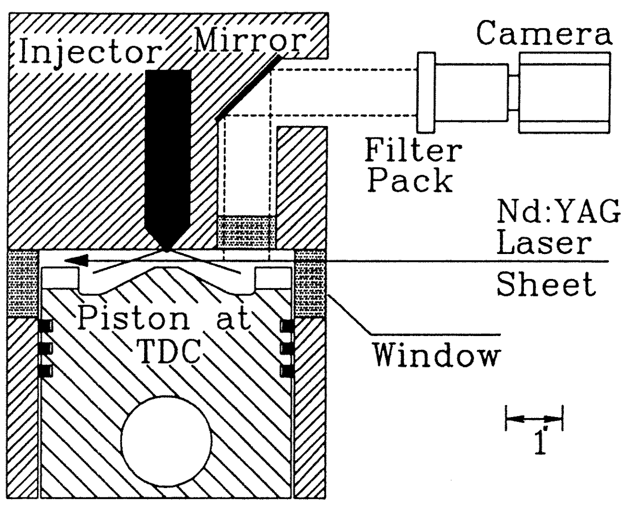

Figure 3 Schematic of the engine's optical configuration.

(diametrically opposed) valve cutouts were enlarged to allow the laser sheet to clear the piston at top dead center (TDC). Self-lubricating Vespel piston rings were used to allow operation with reduced cylinder lubrication. The top compression ring was 3.81 cm (1.5 in.) below the piston rim, 1.25 cm (0.49 in.) lower than the top compression ring of the stock piston. This was necessary to avoid contact between the ring and the quartz window.

3) One of the two exhaust valves was replaced by a 3.34 cm (1.315 in.) diameter quartz window. The intake valves were unchanged to preserve the engine intake event. The effect of one less exhaust valve on air flow near TDC should be small. Also for the 600 rpm engine speed used in this study the effect of removing one exhaust valve should not have a significant effect on residual fraction.

4) A production PT fuel injector was used. In order to be able to view individual spray plumes, however, the 9 hole production cup was replaced with a 4 hole cup, resulting in 4 equally spaced spray plumes. Orientation of the injector was such that the axis of one of the plumes pointed directly at one of the windows in the spacer ring as shown in Fig. 3. The angle between the axis of the spray plume and the cylinder head is nominally 18°.

The engine was connected to a balancing box through a toothed belt and mounted on a spring-mounted isolation pad. The engine speed was controlled through a 75 hp DC dynamometer, while the crankshaft position was monitored by a shaft encoder with 1° resolution. An air compressor supplied pressurized intake air which was dehumidified and heated. The flow rate of intake air was metered by an automatic control-valve/mass-flow-meter feedback system. Surge tanks were installed on both the intake and the exhaust systems.

Optical Set Up

The frequency doubled output (532 nm) of a pulsed Nd:YAG laser was passed through a set of cylindrical and plano-convex lenses to produce a horizontal laser sheet with a thickness on the order of 500 μm and a width of about 5 cm. Laser output was about 0.3 Joules per pulse which resulted in a power level in the laser sheet of about 1.5 x 10^8 W/cm^2. The laser sheet was directed through the window in the spacer ring directly into the spray plume, as shown in Fig. 3. An adjustable mirror permitted the laser sheet to be set at any desired vertical position within the window. The LII signal passes through the window in the cylinder head and is then filtered before entering an intensified CID camera. The filters, required to suppress background luminosity and elastic scattering of the laser, consisted of two 450 nm short wavelength pass interference filters, one BG39 Schottglass short wavelength pass color-glass filter and a 532 nm laser mirror. The camera had a resolution of 240 by 388 pixels and was connected to a frame grabber in an IBM AT type computer.

Synchronization between the engine, laser, camera, and intensifier gate was controlled by a second IBM AT type computer [8] and a digital delay generator. The laser was fired once each 720° engine cycle yielding a 5 hz repetition rate at the 600 rpm engine speed used in this study. The 80 ns gate of the camera intensifier was positioned so that the intensifier was operating at full gain when the laser pulse occurred. This synchronization system could be adjusted so that an LII image could be obtained at any crank angle desired. Images were acquired and stored in the computer's memory in sets of 15 at a rate corresponding to one image every other combustion cycle.

RESULTS AND DISCUSSION

For all the results presented in this paper, the engine was operating under the conditions which are listed in Table 2. Note that the air fuel ratio was 140, corresponding to a low load operating condition. This load condition was selected to minimize the optical thickness of the soot in the spray plume and therefore to minimize the effects of laser attenuation and LII signal trapping, mentioned above. It should be noted that the problems of soot attenuation of the laser and signal are not unique to LII, but are inherent with almost any optical technique (i.e., Mie scattering or laser-induced fluorescence) used in a strongly sooting environment.

Table 2. Operating Conditions

Engine speed	600 rpm
Intake temperature	150 C
Intake air flow	180 lbs/hr
Intake pressure	2 bar absolute
Air/Fuel ratio	140
Start of injection	TDC

For the conditions studied, attenuation of the laser intensity across the image plane is not thought to be a significant problem for two reasons. First, Mie scattering images obtained using the same optical setup and laser power showed a strong signal (from the liquid fuel) on the injector side of the spray plume, indicating that the laser power was significant after penetrating the sooting part of the plume. Second, the laser power density used was 15 times the nominal threshold level of 10^7 W/cm^2 required to maintain soot particles at their vaporization temperature, 4500 K. Attenuation of the laser intensity by the soot would have to be greater than this factor of 15 to significantly reduce the incandescence signal.

Even at this low load condition, trapping of the LII signal can be a problem. Transmission measurements across the entire vertical thickness of the combusting spray plume showed that near the center of the plume the LII signal was completely obscured by soot or liquid fuel at some crank angles during some engine cycles, though for most conditions obscuration was only partial. These measurements provided a worst case test since they measured obscuration across the entire plume, whereas laser sheet was not lowered below about half the plume thickness (1.9 cm, 0.75 in.) due to interference with the piston. Most of the images presented in this paper were taken in the plane 1.27 cm (0.5 in.) below the cylinder head. This plane is above the centerline of the spray, and we believe that obscuration did not severely affect these images.

Figure 4 shows samples of 2-D soot images taken in the horizontal plane 1.27 cm (0.5 in.) below the cylinder head at 17 degrees after top dead center (ATDC). These images were taken in different engine cycles. In these images, the 3.8 cm (1.3 in.) diameter field of view through the window in the cylinder head is indicated by the black circles. The injector tip is located outside the field of view (see Fig. 3) in the lower left hand corner, with the injector oriented in such a way that the axis of one of the spray plumes passed directly through the center of the field of view from the lower left hand corner to the upper right hand corner. Regions of high soot concentration appear black, regions of lower soot concentration appear in shades of gray, and regions where the soot concentration was zero or too low to be detected appear white.

These images show that the soot is not distributed uniformly. On the contrary, we observed sharply defined, irregular regions of high soot concentration. To better show how sharply divided these regions are, intensity cross sections along the horizontal line drawn through each image are plotted in the lower half of the figure. Shown between the two intensity plots is the gray scale mapping of the intensity used in the images. As can be seen in this figure, sharp gradients separate the regions of high and low image intensity, which correspond to regions of high and low soot concentration.

A sequence of images, taken in the plane 1.27 cm (0.5 in.) below the cylinder head is shown in Fig. 5. Although significant cycle-to-cycle variation occurred (see Fig. 4), comparisons of images from many cycles showed a definite trend in the change of soot concentration with time. The images presented in Fig. 5 were selected from separate engine cycles and arranged in this fashion to portray the change of the soot distribution with time. As the combustion progresses and as regions of high soot concentration are convected both across the chamber and perpendicular to the laser sheet, the overall distribution of soot changes significantly. What does not

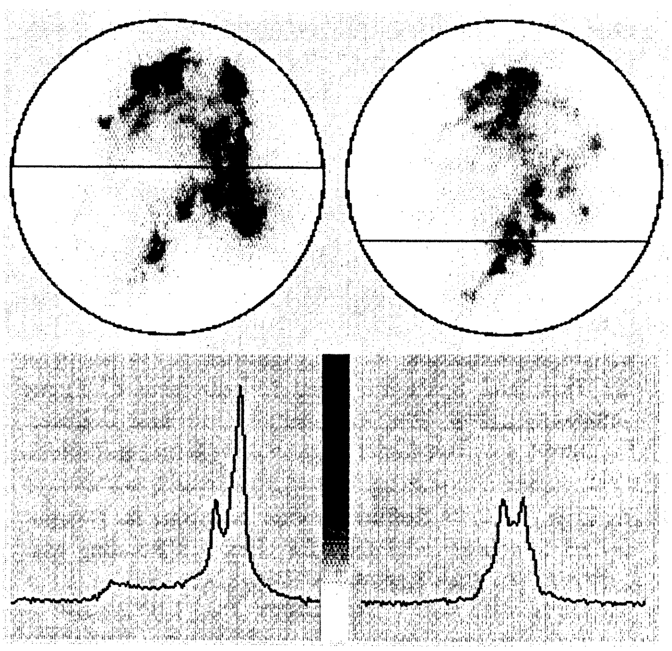

Figure 4 Typical 2-D soot images obtained using LII with signal intensity profiles. Images from two different engine cycles are shown. Dark regions correspond to regions of high signal intensity. (The gray scale mapping of LII signal intensity is shown between the two plots.) The location is 1.27 cm (0.5 in.) below the cylinder head, 17° ATDC.

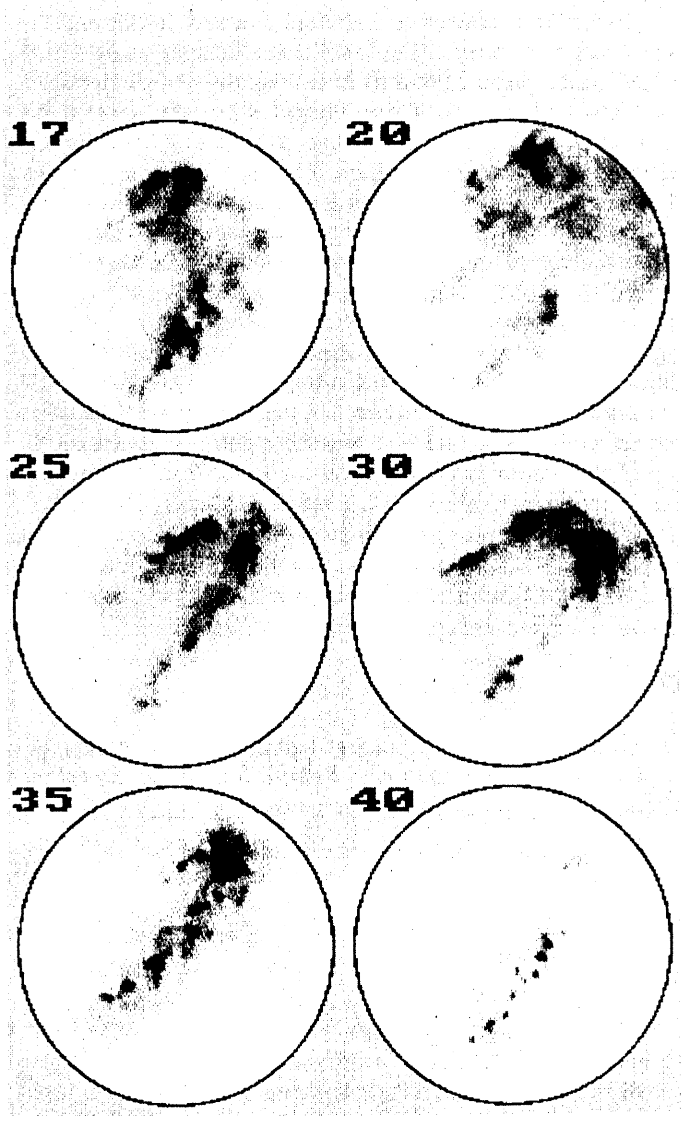

Figure 5 Soot image sequence in the plane 1.27 cm (0.5 in.) below the cylinder head. The number to the upper left of each image denotes the crank angle degrees ATDC.

Figure 6 LII soot images from two different engine cycles. Image location is 1.9 cm (0.75 in.) below the cylinder head, 17° ATDC.

change, however, is the non-uniform distribution of the soot. Even very late in the combustion cycle, sharply defined regions of soot can be observed.

To further examine the distribution of soot in this engine, we raised and lowered the laser sheet. Images taken at 17 ATDC in the plane 1.9 cm (0.75 in.) below the cylinder head are shown in Fig. 6. These images show the soot to be concentrated in a horseshoe shaped region. A comparison between these images and those of flame luminosity shows that this high-soot region is located near the periphery of the combusting spray plume. The reason for the lack of LII signal in the center of the plume is not known, since this is the region where obscuration of the LII signal is most severe, and the plane of the laser sheet is now lower in the plume. If signal obscuration were not an issue, this image would indicate that combustion plume is behaving like a typical diffusion flame with soot present only around the surface and the central region likely being fuel rich with no significant reactions. If signal obscuration is very high, however, soot could be present across this region while the LII signal is blocked. Interpretation of the images becomes an even greater problem at higher fuel loads. Methods for mitigating this obscuration which limits the application of LII and other laser-based diagnostics in diesel engines are currently being studied.

CONCLUSIONS

Using 2-D imaging of laser-induced incandescence the spatial distribution of soot was studied in a DI diesel engine. The following observations were made:

- LII is a promising technique for studying soot distribution in diesel engines.
- This technique allows imaging of soot in the presence of liquid droplets.
- Spatially non-uniform obscuration of the signal by soot located between the laser sheet and the camera can severely affect the measurements. This makes it very difficult to interpret measurements obtained under high sooting conditions.
- The images show strong spatial non-uniformities in soot distribution.
- Regions of low soot concentration and high soot concentration are separated by sharp gradients.
- The scale of the high soot concentration regions is on the order of several millimeters.
- Regions of high soot concentration remain even near the end of the combustion period.

ACKNOWLEDGEMENTS

The authors would like to thank Bill Flower, Bob Green, Roy Primus, Pat Flynn, and Gary Hubbard for many helpful discussions, John Schroeder and Henry Ng for their technical assistance, and Fred Bracco for his help during the conception of this project. The measurements were performed at the Combustion Research Facility at Sandia National Laboratories. The authors thank Cummins Engine Company, Sandia National Laboratories, and the U.S. Department of Energy, Energy Conversion and Utilization Technologies Program for supporting this work.

REFERENCES

1. Weeks, R.W. and Duley, W.W., "Aerosol-Particle Sizes from Light Emission During Excitation by TEA CO_2 Laser Pulses," Journal of Applied Physics, Vol. 45, No. 10, pp. 4661-4662, October 1974.
2. Eckbreth, A.C., "Effects of Laser Modulated Particulate Incandescence on Raman Scattering Diagnostics," Journal of Applied Physics, Vol 48, No. 11, pp 4473-4479, November 1977.
3. Melton, L.A., "Soot Diagnostics Based on Laser Heating," Applied Optics, Vol. 23, No. 13, pp 2201-2208, July, 1984.
4. Dasch, C.J., "New Soot Diagnostics in Flames Based on Laser Vaporization of Soot," Twentieth Symposium (International) on Combustion, The Combustion Institute, pp 1231-1237, 1984.
5. Dasch, C.J., "Continuous-wave probe laser investigation of laser vaporization of small soot particles in a flame," Applied Optics, Vol. 23, pp 2209-2215, 1984.
6. Dasch, C.J., "Spatially resolved soot-absorption measurements in flames using laser vaporization of particles," Optics Letters, Vol 9, pp 214-216, 1984.
7. Matsui, Y., Kamimoto, T., and Matsuoka, S., "A Study on the Time and Space Resolved Measurement of Flame Temperature and Soot Concentration in a D.I. Diesel Engine by the Two-Color Method," SAE paper 790491, 1979.
8. zur Loye, A.O., "A Software-Based Controller for Generation of Synchronized Pulses for Use with Rotating Machinery," SANDIA Report SAND89-8247, 1989.